Biological Sciences – Biophysics and Computational Biology

Prebiotic amino acids bind to and stabilize prebiotic fatty acid membranes

Caitlin E. Cornell[a], Roy A. Black[a,b,1], Mengjun Xue[a], Helen E. Litz[a], Andrew Ramsay[a], Moshe Gordon[a], Alexander Mileant[c,d], Zachary R. Cohen[a], James A. Williams[c], Kelly K. Lee[c], Gary P. Drobny[a], and Sarah L. Keller[a,1]

[a] Dept. of Chemistry, University of Washington, Seattle WA 98195 USA
[b] Dept. of Bioengineering, University of Washington, Seattle WA 98195 USA
[c] Dept. of Medicinal Chemistry, University of Washington, Seattle WA 98195 USA
[d] Biological Structure, Physics, and Design Graduate Program, University of Washington, Seattle WA 98195 USA

[1]Corresponding authors
blackr5@uw.edu, 206-713-4603
slkeller@chem.washington.edu, 206-543-9613

Short title: Amino acids stabilize prebiotic membranes

ABSTRACT

The membranes of the first protocells on the early Earth were likely self-assembled from fatty acids. A major challenge in understanding how protocells could have arisen and withstood changes in their environment is that fatty acid membranes are unstable in solutions containing high concentrations of salt (such as would have been prevalent in early oceans) or divalent cations (which would have been required for RNA catalysis). To test whether the inclusion of amino acids addresses this problem, we coupled direct techniques of cryo electron microscopy and fluorescence microscopy with techniques of nuclear magnetic resonance spectroscopy, centrifuge filtration assays, and turbidity measurements. We find that a set of unmodified, prebiotic amino acids binds to prebiotic fatty acid membranes and that a subset stabilizes membranes in the presence of salt and Mg^{2+}. Furthermore, we find that final concentrations of the amino acids need not be high to cause these effects; membrane stabilization persists after dilution, as would have occurred during the rehydration of dried or partially-dried pools. In addition to providing a means to stabilize protocell membranes, our results address the challenge of explaining how proteins could have become co-localized with membranes. Amino acids are the building blocks of proteins, and our results are consistent with a positive feedback loop in which amino acids bound to self-assembled fatty acid membranes, resulting in membrane stabilization, leading to more binding in turn. High local concentrations of molecular building blocks at the surface of fatty acid membranes may have aided the eventual formation of proteins.

Keywords: Prebiotic, fatty acid, membrane, amino acids, protocell, origins of life, hydrothermal pools

SIGNIFICANCE STATEMENT

How did the first cells on Earth arise? In a minimal cell, a membrane separates proteins and RNA from the surrounding aqueous environment. Cell-like membranes spontaneously assemble from simple prebiotic surfactants called fatty acids. However, fatty acid membranes are unstable in solutions containing salts that were likely present in environments of the early Earth. We find that amino acids, the building blocks of proteins, bind to fatty acid membranes and stabilize them against salts. Moreover, enhanced stabilization persists following dilution as would occur when a dehydrated pool re-fills with water – a likely setting for the emergence of cells. In addition to explaining how the first membranes were stabilized, our findings answer how key components of the first cells co-localized.

INTRODUCTION

In a minimal cell, a membrane sequesters proteins and RNA components from the surrounding aqueous solution. Prebiotic membranes would have spontaneously self-assembled from fatty acids (1, 2), which are known to be generated by abiotic reactions and delivered to Earth by meteorites (3, 4). However, fatty acid membranes are unstable in solutions containing salt at concentrations > 200 mM or divalent cations at low millimolar concentrations (5). This presents a significant challenge in establishing the plausibility that the first protocell membranes were comprised of fatty acids because salt would have been prevalent in early oceans (6) and pools and because Mg^{2+} (or Fe^{2+}) is essential for RNA catalysis (7, 8). Although glycerol monoesters (9, 10), long-chain alcohols (11, 12), decylamine (13, 14), and citrate (15) increase the stability of fatty acid vesicles (cell-like structures that separate an interior volume from the bulk solution), the prebiotic availability of these agents in sufficient quantities is uncertain (16). These observations lead to the question: what molecules that were likely found in prebiotic pools and oceans might interact with and stabilize fatty acid membranes? Amino acids are the building blocks of proteins, and ten amino acids are deemed prebiotic (17-20). These molecules are excellent candidates for stabilizing agents of fatty acid membranes.

An additional challenge in explaining the origin of protocells is accounting for the co-localization of proteins, RNA, and membranes as a single unit. A prevalent view is that these three structures were formed through separate and independent processes, followed by a random event that led to their co-localization. We have proposed an alternate, auto-amplification scenario in which fatty acid vesicles bound and concentrated the building blocks of proteins and RNA, which in turn stabilized fatty acid vesicles, leading to further binding of the building blocks (21, 22). If the resulting conformational constraints and increased local concentration of the building blocks facilitated formation of proteins and RNA, then the co-localization of these macromolecules with fatty acid membranes would be explained. We previously reported results with RNA bases and ribose that support part of this scenario (21). Here we seek to complete the picture by investigating interactions between amino acids and fatty acid membranes to show that all of the major components of protocells could have self-assembled into a single unit.

Our focus is on molecules that are prebiotically plausible. Previous studies have shown evidence for interactions between fatty acid vesicles and non-prebiotic amino acids and peptides (23-27). Here, we use decanoic acid as our fatty acid rather than longer-tailed versions that produce more stable membranes but are less prebiotically plausible. We choose unmodified prebiotic amino acids rather than versions altered to optimize specific reactions. We interrogate interactions between the decanoic acid membranes and the amino acids with multiple techniques: cryo electron microscopy (cryo TEM), fluorescence microscopy, nuclear magnetic resonance spectroscopy, centrifuge filtration assays, and turbidity measurements.

We find that several amino acids bind to fatty acid membranes and that a subset stabilize fatty acid membranes in the presence of salt and Mg^{2+}. Moreover, we find that an amino acid's stabilization of the membrane persists after mixing and dilution to lower overall concentrations, alleviating the need for consistently high concentrations. Together, these results explain how protocells could have endured in the presence of salt and Mg^{2+} and provide a plausible mechanism by which the building blocks of proteins could have co-localized with early membranes.

RESULTS

Amino acids bind to decanoic acid vesicles

Evidence that amino acids bind to decanoic acid vesicles emerges from two types of experiments: diffusion NMR spectroscopy and filtration assays. Diffusion NMR exploits the fact that when molecules in solution bind to surfaces, even transiently, the apparent rate at which they diffuse decreases. Of the ten amino acids that are widely regarded as prebiotically plausible (17-20), we chose three characteristic structures to investigate with this technique: glycine has no side chain, leucine has a hydrophobic side chain, and serine has a hydrophilic side chain. The structures of the fatty acid and amino acids we used appear in SI Appendix, Fig. S1, and the experiments are summarized in Table S1. As a positive control, we chose a positively charged amino acid, lysine, which is not considered prebiotic (17-20). Lysine should bind to negatively charged decanoic acid headgroups. We attempted to include aspartic acid (to represent amino acids with acidic side chains), but it was insoluble under our experimental conditions.

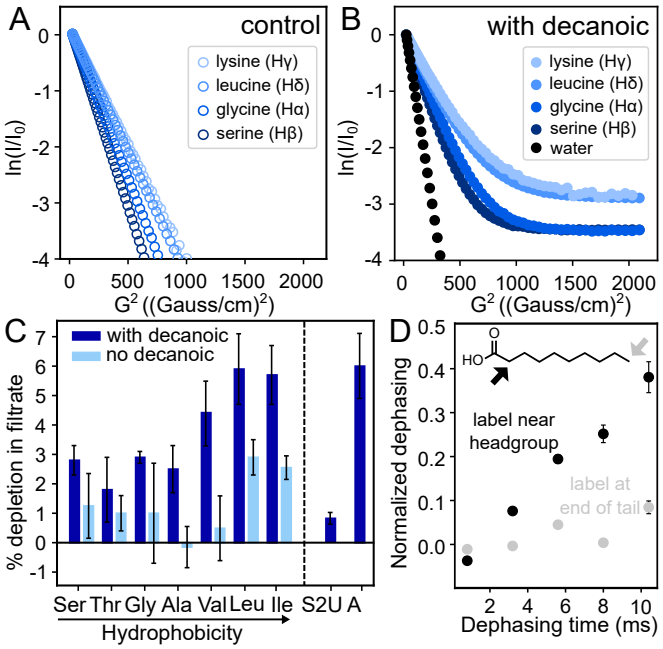

Figure 1. Amino acids bind to fatty acid vesicles. **A.** Lysine, leucine, glycine, and serine diffuse freely in solution with one characteristic diffusion coefficient indicated by a straight line on a plot of the square of the NMR magnetic field gradient strength (G^2, where G is dB/dz in units of Gauss/cm and B is the magnetic field) vs. normalized peak intensity (ln I/I_0). The slope of the line yields the first coefficient in Table 1. **B.** When the amino acids are in decanoic acid solutions containing micelles and vesicles, two slopes (and two diffusion coefficients) are distinguishable. Water, which is a negative control because it is not expected to bind to vesicles, shows only one slope. **C.** Amino acids are retained with decanoic acid vesicles in a centrifugal filtration assay (dark bars). Controls (light bars) were performed in the absence of decanoic acid; given that decanoic acid is a surfactant, controls may represent an overestimate of the

binding to the filtration unit that occurs in the presence of decanoic acid. Error bars represent standard errors of the mean for independent experiments conducted 7 (Ser), 10 (Thr), 5 (Gly), 17 (Ala), 5 (Val), 7 (Leu), 5 (Ile), 3 (thiouracil), 3 (adenine), and 4 (controls) times. The P values for the differences between Ser, Thr, Gly, Ala, Val, Leu, and Ile and their respective controls without decanoic acid are 0.15, 0.65, 0.25, 0.15, 0.04, 0.10, and 0.04 (Student's two-tailed *t* test). The P values for Ser, Thr, Gly and Ala compared to leucine are 0.03, 0.02, 0.06 and 0.03. Thiouracil (S2U) and adenine (A) were insufficiently soluble in the absence of decanoic acid to run controls. The hydrophobicity ranking is from (40). **D.** Leucine and the headgroups of decanoic acid molecules interact within a distance < 5 Å in lyophilized samples. $^{13}C\{^{2}H\}$ REDOR dephasing occurs when decanoic acid is labeled near its carboxyl group (filled symbols) and not when labeled at the terminal methyl group (open symbols).

On their own in solution, amino acids move freely with single, fast diffusion coefficients, as shown in Fig. 1A and Table 1. When the amino acids are in the presence of decanoic acid vesicles, separate fast and slow sets of coefficients appear, which arise from the bi-exponential curves in Fig. 1B. The reason the fast coefficients in Fig. 1B (with decanoic acid) are slightly lower than in Fig. 1A (without decanoic acid) is likely that decanoic acid solutions have a higher bulk viscosity than water (28). The slow set of coefficients is due to binding of amino acids to decanoic acid surfaces, in accordance with other NMR diffusion results (29). This binding could be due to amino acids associating with the outer surface of vesicles and micelles (whose structures appear in SI Appendix, Fig. S1), traversing the vesicle membrane, or associating with the inner surface of vesicles. Within Fig. 1B, stronger binding is reflected in a higher y-intercept (the intensity) for the second slope; hence, leucine (which is hydrophobic) and lysine (which is positively charged) bind more strongly to decanoic acid vesicles than serine and glycine do.

	Diffusion Coefficient (m^2/s)		
	No vesicles (fast)	With vesicles (fast)	With vesicles (slow)
Water	1.692×10^{-10}	1.563×10^{-10}	Not applicable.
Serine	6.373×10^{-10}	6.132×10^{-10}	1.8×10^{-12}
Glycine	7.645×10^{-10}	7.397×10^{-10}	1.0×10^{-12}
Leucine	5.210×10^{-10}	4.951×10^{-10}	3.0×10^{-12}
Lysine	4.888×10^{-10}	4.580×10^{-10}	1.0×10^{-11}

Table 1. Translational diffusion coefficients for water and for amino acids in solutions with and without decanoic acid vesicles.

Maximum uncertainties are ± 0.63% for water, ± 2.4% for fast coefficients of amino acids, and ± 61% for slow coefficients. The corresponding Table S2 lists values for each experiment and describes how experimental uncertainties were calculated. If uncertainties are neglected, the percent of each amino acid that binds to vesicles is calculated to be 3% for Gly, 3% for Ser, 5% for Leu, and 6% for Lys, in agreement with values in Fig. 1C.

The diffusion coefficients in Table 1 tell us that the new set of (slow) coefficients is not merely due to encapsulation of amino acids within vesicles. In samples without vesicles, leucine's diffusion coefficient corresponds to a length scale of 18 μm within the NMR time scale of 0.3 seconds (via the 1-dimensional diffusion equation $r^2 = 2Dt$, where r is the length, D is the diffusion coefficient, and t is the time). Limiting the length to 10 μm, the approximate size of a decanoic acid vesicle, would yield a diffusion coefficient of 1.7×10^{-10} m^2/s, which is two orders of magnitude greater than for leucine in the presence of vesicles. Additional support that the slow diffusion coefficient is due to binding is that diffusion coefficients for highly mobile (*e.g.* unsaturated) phospholipids across the surface of bilayers have comparable values within uncertainty, on the order of 10^{-12} to 10^{-11} m^2/s (30).

Using an independent test of binding based on centrifugal filtration, we find that the three most hydrophobic amino acids (valine, leucine, and isoleucine) are retained to a greater extent when they are in the presence of decanoic acid vesicles and micelles (Fig. 1C). Retention of the four least hydrophobic amino acids (serine, threonine, glycine, and alanine) is insignificant relative to controls and is significantly less than the retention of leucine. These results support our conclusion that association of amino acids with vesicles is indeed due to binding rather than a nonspecific effect such as encapsulation within vesicles, because encapsulation would yield the same retention in all cases. To quantify the maximum signal that we would expect from nonbinding effects, we repeated the experiment with thiouracil (which differs from the nucleobase uracil by the substitution of a sulfur for an oxygen atom). We chose thiouracil because it is negligibly retained with decanoate micelles, which suggests that its binding to vesicles should be low as well (21). The result, depletion in the filtrate of 0.8 ± 0.2%, indicates that no more than ~1% of the thiouracil is depleted from the filtrate due to encapsulation in vesicles. If some or all of the ~1% is due to binding, the amount encapsulated and unbound is even lower (Fig. 1C). Our positive control, using the same assay for detection, was the nucleobase adenine, which interacts strongly with micelles and vesicles (21). As expected, adenine is strongly retained (Fig. 1C).

Our results in Fig. 1B-C, namely that hydrophobic and positively charged amino acids bind most strongly to fatty acid vesicles, imply that the amino acids' side chains contribute to the binding. We interrogated leucine's mode of interaction with decanoic acid by testing if it interacts with hydrogen atoms close to the headgroup of decanoic acid, with hydrogens at the end of decanoic acid's carbon chain, or both. To conduct this test, we employed rotational-echo double-resonance (REDOR) NMR spectroscopy, which measures the dipolar coupling between ^{13}C and ^{2}H nuclei. $^{13}C\{^{2}H\}$ REDOR is commonly used to probe protein-membrane interactions (31-34). We found that leucine interacts with a hydrogen near the headgroup of decanoic acid, but not at the end of the tail (Fig. 1D, SI Appendix, Fig. S2). Specifically, we lyophilized solutions containing labeled leucine and decanoic acid vesicles. We measured the dephasing of ^{13}C-labeled leucine by two versions of decanoic acid: one ^{2}H-labeled at the 2-carbon that adjoins the carboxyl group and one ^{2}H-labeled at the 10-carbon at the end of the carbon chain. We find significant dephasing in the former case (indicating that the moieties interact over distances <5 Å) and not in the latter.

Amino acids increase vesicle stability against Mg^{2+} and/or NaCl

What significance does binding of amino acids to fatty acid membranes hold for the origins of life on Earth? As described in the introduction, a challenge in constructing a plausible scenario in which the first protocells incorporated fatty acid membranes is that individual, ~10 μm vesicles are unstable in the presence of divalent and monovalent ions (5) that would have been

present in early oceans (6) and pools and, in the case of Mg^{2+} or Fe^{+2}, would have been required for RNA catalysis (7, 8). Here we show cases in which amino acids stabilize individual, large fatty acid vesicles against such cations.

Fig. 2E shows that 10 mM Mg^{2+} converts individual, ~10 μm vesicles into punctate structures (compare with Fig. 2A). The addition of serine or glycine, amino acids that lack hydrophobic side chains, to decanoic acid solutions with Mg^{2+} has an enormous positive effect: these amino acids convert the punctate structures back to intensely bright ~10 μm vesicles (compare Fig. 2B-C with 2F-G). In contrast, the addition of leucine, which has a hydrophobic side chain, provides no protection against the Mg^{2+} (Fig. 2H).

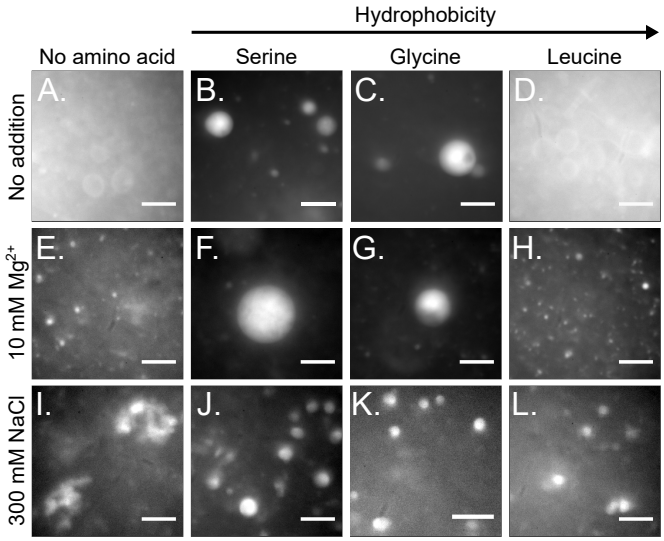

Figure 2. Amino acids can stabilize decanoic acid vesicles against Mg^{2+} and NaCl. **A.** Vesicles ~10 μm in diameter self-assemble in the decanoic acid solution described in the Methods. **B-C.** In the presence of 10 mM serine or glycine, these ~10 μm vesicles appear brighter, consistent with multilamellar structures. Vesicle lumens are aqueous; they can be labeled with calcein, a soluble dye (SI Appendix, Fig. S3). **D.** In contrast, in the presence of 10 mM leucine, ~10 μm vesicles are indistinguishable from those in panel A. **E-H.** When the decanoic acid solutions include 10 mM Mg^{2+}, bright, ~10 μm vesicles are retained if the solutions also contain serine or glycine. In contrast, in solutions without amino acid or in the presence of leucine, micron-scale vesicles are replaced by punctate structures, some of which are smaller vesicles. **I-L.** When 300 mM NaCl is added at room temperature to 80 mM decanoic acid at pH 7.65, vesicles flocculate. After heating the solution to 60 °C to disaggregate the flocs and then cooling to 30˚C, individual ~5 μm vesicles re-form in solutions containing 10 mM serine, glycine, or leucine. In contrast, in solutions without amino acid, flocs re-form. All panels are fluorescence micrographs; scale bars are 10 μm.

We conducted three tests to verify that the ~10 μm vesicles observed in solutions with serine are indeed vesicles rather than oil droplets. First, we showed that with or without Mg^{2+}, the vesicles can encapsulate calcein and retain it through the process of size exclusion chromatography (SI Appendix, Fig. S3 C-D and S4 C-D). In contrast, oil droplets of decanoic acid exclude calcein, so are visually distinct from vesicles (SI Appendix, Fig. S3 G-H). Second,

we showed that the size of individual, free-floating vesicles in the presence of serine and Mg^{2+} does not visibly increase over 24 hours (SI Appendix, Fig. S5 K-L), whereas oil droplets coalesce unless they are on glass surfaces (c.f. (35)). Third, we showed that bulk solutions containing Mg^{2+} (with or without serine) do not separate with a clear layer on the bottom and an oil layer on top, as a solution of oil droplets does (SI Appendix, Fig. S5).

The mechanism by which Mg^{2+} eliminates individual, ~10 μm vesicles presumably involves binding of this cation to the carboxylate headgroups of the membrane. This mechanism forms the basis of three speculations: serine may block the binding of Mg^{2+} through interaction of its side chain hydroxyl group and decanoic acid headgroups; glycine may block it through interaction of its amine with the headgroups (because its amine can rotate relatively freely around the α-carbon); and leucine may fail to block the binding of Mg^{2+} because its side chain orients in the bilayer such that leucine's amine and/or carboxyl group is less accessible to fatty acid headgroups. Although our micrographs clearly show that Mg^{2+} eliminates ~10 μm decanoic acid vesicles, it is difficult to characterize the structures that replace them. At least some of the puncta are consistent with vesicles, but a few approach 1 μm in size, and poor correspondence between puncta labeled with rhodamine 6G and calcein implies that the membranes allow leakage of vesicle contents.

Individual, ~10 μm decanoic acid vesicles are also unstable in the presence of high NaCl concentrations (5). Vesicles flocculate immediately when 300 mM NaCl is added to decanoic acid solutions at room temperature, whether or not the solutions contain amino acids. However, when these solutions contain serine, glycine, or leucine (amino acids that span a wide range of hydrophobicities) and are temperature cycled, a striking, beneficial change occurs. Heating the flocs to 60 ˚C causes them to disaggregate, and as the solutions cool to 30-32 ˚C, flocs re-form in solutions without amino acids (Fig. 2 I), whereas serine, glycine, and leucine reduce flocculation (SI Appendix, Fig. S5 G-J), retaining many discrete, bright vesicles (Fig. 2 J-L). To confirm that these structures are vesicles rather than oil droplets, we verified that they do not behave as oil droplets: they do not float to the top of a solution in a separate layer, and they do not visibly grow over 24 hours (SI Appendix, Fig. S5). Our results are important because they imply that amino acids could have enabled large, individual decanoic acid vesicles to form in early oceans or drying pools, in which salt levels may have been high (6).

Vesicle stability against Mg^{2+} correlates with an increase in lamellarity

Two lines of direct evidence imply that an amino acid's success in stabilizing individual, ~10 μm vesicles in the presence of Mg^{2+} correlates with an increase in the number of lamellae in each vesicle. The first evidence follows from the fluorescence micrographs in Fig. 2A-C and 3A-B, which show that individual vesicles are brighter in the presence of serine and glycine, suggesting that more decanoic acid membranes are present in each vesicle. As noted above, we know that the bright structures are not oil droplets because they have lumens that encapsulate calcein, whereas oil droplets exclude calcein (SI Appendix, Fig. S3).

Additional evidence that serine increases lamellarity comes from cryo TEM, which interrogates submicron structures. Without amino acids, > 80% of submicron vesicles are paucilamellar, with ≤ 3 nested vesicles (Fig. 3D and 3F). Only ~10% of vesicles have ≥ 4 lamellae. When vesicle solutions include serine, which stabilizes vesicles against Mg^{2+}, the percentage of vesicles with ≥ 4 lamellae jumps to > 30% (Fig. 3E and 3F). The increase in lamellarity induced by serine persists following the addition of Mg^{2+} (SI Appendix, Fig. S6).

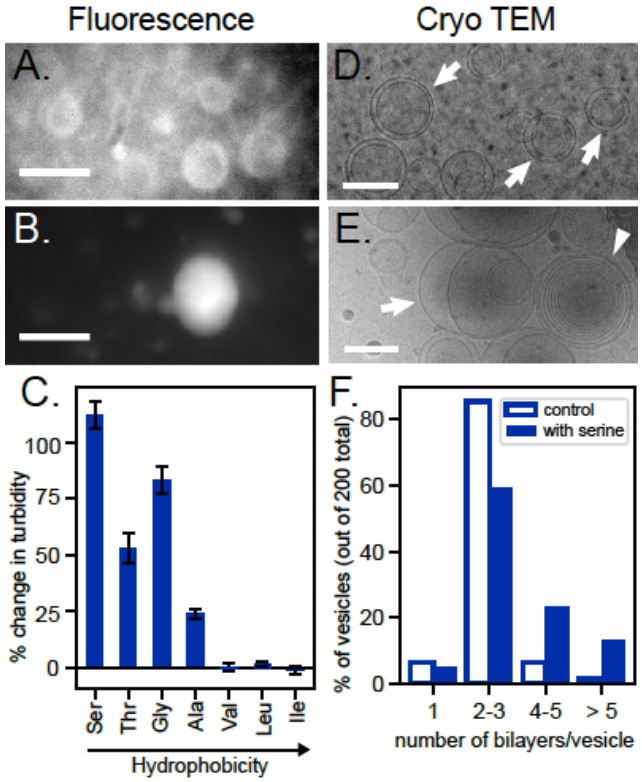

Figure 3. Serine increases vesicle lamellarity. **A-B**. Vesicles in the decanoic acid solution were imaged by fluorescence microscopy without (A) and with (B) 10 mM serine. Panels A and B are cropped sections of Fig. 2A-B, with linear contrast enhancement. Scale bars are 10 μm. **C.** Amino acids were dissolved in the decanoic acid solution to yield 10 mM solutions. Turbidity was measured by absorbance 30 minutes later. pH was constant. The graph shows the change in turbidity relative to a control without amino acid. **D-E.** Vesicle structure in decanoic acid solutions without (D) and with (E) 10 mM serine was imaged by cryo TEM. Arrows indicate paucilamellar vesicles; wedges indicate multilamellar vesicles. Scale bars are 100 nm. Cryo TEM records images of vesicles that are two orders of magnitude smaller than fluorescence microscopy does because vesicles >300 nm are not retained on TEM grids. **F.** The fraction of vesicles with >3 lamellae is higher in decanoic acid solutions containing serine.

An increase in lamellarity is also beneficial in the context of protocell growth and division. As Joyce and Szostak have noted: "In contrast to the behavior of multilamellar vesicles, large unilamellar vesicles are fragile and tend to rupture with extensive loss of contents under shear stress. These features combine to make multilamellar vesicles … attractive as a means of simple, environmentally driven cycles of growth and division, requiring only episodic delivery of additional amphiphiles and a moderately turbulent environment" (16).

The amino acid leucine presents an interesting counterpoint. Leucine does not protect large, ~10 μm vesicles against Mg^{2+} (Fig. 2). However, leucine does protect against flocculation of

vesicles in the presence of NaCl. Therefore, stabilization against flocculation by NaCl does not appear to rely upon an increase in the number of lamellae.

Serine, glycine and the other relatively hydrophilic amino acids increase turbidity

Above, we showed that an increase in the number of lamellae of decanoic acid vesicles correlates with an increase in vesicle brightness when solutions contain serine (Fig. 3). To establish a correlation that can be measured with a higher-throughput technique, we also evaluated solution turbidity, specifically, solution absorbance at 490 nm. As summarized in Table S1, vesicle brightness (which we measured for solutions containing serine, glycine, and leucine) correlates with turbidity: the highest turbidities are observed when the four most hydrophilic amino acids (serine, threonine, glycine, and alanine) are mixed with the decanoic acid solution (Fig. 3C).

In these turbidity experiments, the decanoic acid solution was added to solid amino acids. Mineral surfaces (36) and ionic strength (37) are known to affect vesicle formation. To test whether the high turbidity of solutions containing the more hydrophilic amino acids results from interactions of the decanoic acid with the surfaces of the solid amino acid or from altered conditions (pH or ionic strength) in the vicinity of the dissolving amino acid, we repeated our experiments by adding amino acids as concentrated solutions rather than solids. We found that amino acids added as solutions produce the same results as when amino acids are added as solids: turbidity increases and the most hydrophilic amino acid produces the highest increase (Fig. S7).

Increases in solution turbidity due to amino acids can be long-lived and can arise at low concentrations. For example, when decanoic acid solutions are prepared with 10 mM serine, elevated turbidity persists at least four days (SI Appendix, Fig. S8), and a significant increase occurs with serine concentrations as low as 1.25 mM (SI Appendix, Fig. S9). The cryo TEM images in Fig. 3D-E suggest that the serine-induced increase in turbidity is due to an increase in vesicle lamellarity. This interpretation is consistent with a recent theoretical analysis predicting a strong effect of lamellarity on turbidity (38). We rule out that the increased turbidity is due to oil drops forming (SI Appendix, Fig. S3) or a decrease in the minimum concentration at which decanoic acid forms vesicles (SI Appendix, Fig. S10). In addition, we do not observe a significant increase in the size of individual vesicles, either by fluorescence microscopy (Fig. 2 and SI Appendix, Fig. S3), or by dynamic light scattering analysis of the apparent hydrodynamic diameter (which was 206 nm for decanoic acid vesicles without amino acid, 205 nm with 10 mM serine). We know that the mechanism by which serine (or any other amino acid that we tested) increases lamellarity and turbidity is not through a change in solution pH because the pH values were the same before and after the addition of amino acid.

Amino acids plausibly increase vesicle lamellarity in pools undergoing cycles of drying and wetting

Damer and Deamer propose that protocells arose in pools undergoing cycles of drying and wetting (39). Concentrations of amino acids and decanoic acid in these pools could have changed in at least two scenarios. In the first scenario, all solutes in a pool could have fully dried together and then have been rehydrated simultaneously. Fig. 4A shows that under these conditions, the three relatively hydrophilic amino acids increase turbidity (and, presumably, the number of lamellae in each vesicle), just as in solutions that are not subjected to drying (Fig. 3C). Therefore, the amino acids' beneficial effects on vesicles persist through periods of drying and wetting.

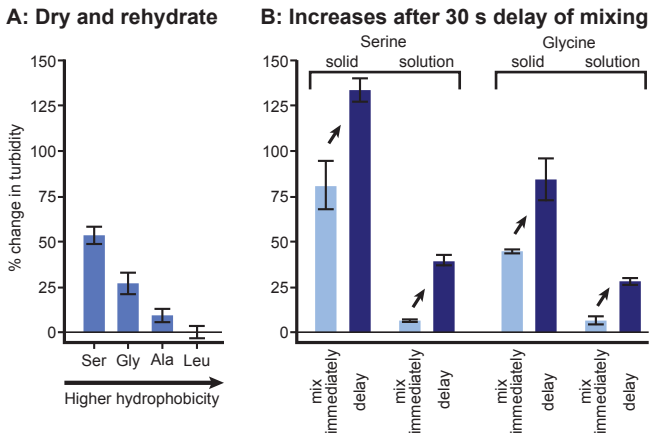

Figure 4. Amino acids increase turbidity of vesicle solutions in two scenarios that recapitulate pools undergoing cycles of drying and wetting. **A.** Drying and rehydration of the decanoic acid solution containing amino acids results in elevated turbidity (absorbance at 490 nm) relative to a solution without amino acids. Error bars show standard error of the mean for four experiments with glycine, alanine, and serine and show average error for two leucine experiments. **B.** Delayed mixing of decanoic acid solutions and amino acid results in higher turbidity, even when final concentrations are constant. The result holds equally well when the amino acid is a solid and when it is in solution. In "solid" samples, the decanoic acid solution was added to a test tube containing solid amino acid such that the final amino acid concentration was 10 mM. In "solution" samples, 10 µL of 1 M amino acid in 50 mM sodium phosphate at pH 6.83 (or the buffer alone) was placed on top of 990 µL of the decanoic acid solution. For both types of samples, mixing by vortexing occurred either immediately or after a delay of 30 seconds. Error bars show average error for duplicate samples.

In the second scenario, the concentration of amino acid relative to decanoic acid could have been transiently elevated. For example, a pool containing amino acids could have partially or completely dried and then fluid containing decanoic acid vesicles could have flowed in. Complete mixing would not have occurred immediately, so the concentration of amino acid would have been high within a boundary layer in contact with the dried or partially dehydrated material. The turbidity experiments in Fig. 3C and SI Appendix, Fig. S7 reproduce this scenario *in vitro* through the addition of vesicle solutions to solid amino acids or by the deposition of a concentrated amino acid solution on a vesicle solution, with a brief delay before mixing.

To determine whether the delay is required for the increased turbidity in the second scenario, we repeated the experiments in parallel with samples that were mixed immediately. The solutions mixed after a delay were indeed more turbid (and presumably contained more multilamellar vesicles) than solutions that were mixed immediately (Fig. 4B), whether the amino acid was serine or glycine. It is important to note that all final concentrations were equivalent, whether the solutions were mixed immediately or after a delay. These results imply that vesicle structures that form during a period of transiently high amino acid concentration, established either as the amino acid dissolves from a solid or as it diffuses from a concentrated solution, persist after dilution caused by mixing. In other words, systems of amino acids and fatty acid

vesicles require a long time to reach equilibrium, even when the vesicles are composed of dynamic molecules like decanoic acid and even when solutions are mixed by vortexing.

Overall, the implication of the results in this section is that amino acids could plausibly have had large effects on protocell structure even if they were at low abundance; amino acids merely needed to be transiently held at higher concentrations, as could have occurred in pools undergoing dehydration and rehydration.

DISCUSSION AND CONCLUSIONS

We used multiple techniques to find that a set of unmodified, prebiotic amino acids binds to decanoic acid membranes and stabilizes large, ~10 μm vesicles in the presence of Mg^{2+} or NaCl. These results are important for two reasons: (1) they help explain how simple prebiotic vesicles could have survived in the presence of divalent cations and salt, and (2) they help explain how the building blocks of biological polymers co-localized with early membranes. In a prebiotic scenario, several types of small molecules likely bound to fatty acid membranes, with varying affinities and different contributions toward stabilizing the large vesicles. Because we found dramatic differences in the consequences of binding (*e.g.* serine and glycine preserved ~10 μm vesicles in the presence of Mg^{2+} whereas leucine did not), large vesicles with a distinct repertoire of bound amino acids could have emerged even if most amino acids had equal binding affinities.

Our fluorescence microscopy, cryo TEM and turbidity data suggest that serine and glycine (amino acids that lack hydrophobic sidechains) stabilize individual large, ~10 μm fatty acid vesicles against Mg^{2+} by increasing the number of lamellae. In contrast, an amino acid that has a hydrophobic side chain (leucine) does not protect the membranes from Mg^{2+} and does not increase vesicle lamellarity (based on fluorescence microscopy and turbidity).

To our knowledge, no other researchers have previously addressed the question of whether prebiotic compounds that stabilize prebiotic fatty acid membranes also increase lamellarity. Monoacyl glycerols and long-chain alcohols probably increase membrane stability by hydrogen bonding with fatty acid headgroups (10, 11). Membrane stabilization by amino acids may also entail hydrogen bonding, particularly in the cases of serine and threonine since the sidechain of each bears a hydroxyl group. However, serine does not lower the critical vesicle concentration whereas monoacyl glycerols and long-chain alcohols do (5, 10, 11). Several other mechanisms of membrane stabilization have been proposed, but none explain our results in full. Citrate increases membrane stability by chelating Mg^{2+} (15); the structures of the amino acids we tested do not suggest chelation as a likely mechanism. Decylamine presumably stabilizes membranes via an electrostatic interaction with fatty acid headgroups (13). This mechanism may also be relevant to amino acids given that the amine group should be positively charged under conditions typically employed for formation of fatty acid vesicles. Since membranes that contain a mixture of amphiphiles are more stable than pure membranes (5, 9-12), it will be interesting to determine whether amino acids stabilize large, ~10 μm vesicles of mixed composition in addition to vesicles of decanoic acid alone.

Our results (summarized in Table S1) are particularly compelling in the context of the hypothesis that protocells arose in pools undergoing cycles of drying and rehydration (39). Such cycles would have produced transiently high concentrations of amino acids. We find that transiently high serine and glycine concentrations cause increases in the turbidity of a decanoic acid solution (a correlate of lamellarity) that persist following dilution. Our results open up

exciting research questions about chemical reactions that would enable the next stage of protocell evolution – does self-assembly of vesicles and amino acids increase synthesis of peptides, and is the system sufficiently robust to support divalent cation-dependent ribozyme activity? Moreover, these discoveries reinforce our previous report that RNA bases bind to and stabilize fatty acid membranes (21). Taken together, those findings and the results reported here support a coherent scenario in which aggregates of fatty acids, which would have spontaneously self-assembled, bound the building blocks of RNA and proteins (nucleobases, ribose, and amino acids), generating the concentration and conformational constraints required for abiotic synthesis of RNA and protein.

METHODS

Decanoic acid solution. Decanoic acid was dissolved, with heating, in 190 mM NaOH to yield a 180 mM stock solution. This stock, 0.5 M monosodium phosphate, and 4 M NaCl were diluted into water to yield a solution of 50 mM decanoic acid, 30 mM sodium phosphate, and 100 mM NaCl. The pH was then adjusted to 6.83 by adding a small volume of 1 M HCl.

Diffusion NMR. Pulsed field gradient nuclear magnetic resonance (PFG-NMR) experiments were performed on a Bruker Avance III 700 MHz NMR instrument with a 5 mm Broadband Observe (BBO) probe at 25 °C.

Filtration assay. Solutions were placed in an Amicon Ultra-4 3K filter and centrifuged in a swinging bucket centrifuge at 3,000 *g* for 10 min at 21 °C.

Turbidity. Turbidity was measured by determining absorbance at 490 nm.

A detailed description of materials and methods is provided in the SI Appendix.

ACKNOWLEDGEMENTS

The Keller and Drobny laboratories were supported by NASA grant NNX17AK86G (Exobiology). K.K.L. and J.A.W. were supported by NIH grant R01-GM099989. C.E.C. and A.M. were funded by the National Institutes of General Medical Sciences of the National Institutes of Health under award T32GM008268 (to C.E.C.) and T32-GM007750 (to A.M.). M.G. and A.R. were supported as undergraduate researchers by National Science Foundation grant MCB-1402059 to S.L.K. We thank our anonymous reviewers for their particularly careful reading of our manuscript and for their in-depth comments.

REFERENCES

1. Deamer D, Dworkin JP, Sandford SA, Bernstein MP, & Allamandola LJ (2002) The first cell membranes. *Astrobiology* 2:371-381.
2. Morigaki K & Walde P (2007) Fatty acid vesicles. *Curr. Opin. Coll. Int. Sci.* 12:75-80.
3. Proskurowski G*, et al.* (2008) Abiogenic hydrocarbon production at Lost City hydrothermal field. *Science* 319:604-607.
4. Lawless J & Yuen G (1979) Quantification of monocarboxylic acids in the Murchison carbonaceous meteorite. *Nature* 282:396-398.

5. Monnard P-A, Apel C, Kanavarioti A, & Deamer D (2002) Influence of ionic inorganic solutes on self-assembly and polymerization processes related to early forms of life: implications for a prebiotic aqueous medium. *Astrobiology* 2:139-152.
6. Knauth LP (2005) Temperature and salinity history of the Precambrian ocean: implications for the course of microbial evolution. *Palaeogeography, Palaeoclimatology, Palaeoecology* 219:53-69.
7. Szostak JW (2012) The eightfold path to non-enzymatic RNA replication. *J. Syst. Chem.* 3:2-1 - 2-14.
8. Jin L, Engelhart AE, Zhang W, Adamala KP, & Szostak JW (2018) Catalysis of template-directed nonenzymatic RNA copying by Iron(II). *J. Am. Chem. Soc.* 140:15016-15021.
9. Chen IA, Salehi-Ashtiani K, & Szostak JW (2005) RNA catalysis in model protocell vesicles. *J. Am. Chem. Soc.* 127:13351-13355.
10. Maurer S, Deamer D, Boncella J, & Monnard P-A (2009) Chemical evolution of amphiphiles: Glycerol monoacyl derivatives stabilize plausible prebiotic membranes. *Astrobiology* 9:979-987.
11. Apel CL, Deamer DW, & Mauntner MN (2002) Self-assembled vesicles of monocarboxylic acids and alcohols: conditions for stability and for the encapsulation of biopolymers. *Biochim. Biophys. Acta* 1559:1-9.
12. Mansy SS & Szostak JW (2008) Thermostability of model protocell membranes. *Proc. Natl. Acad. Sci. U.S.A.* 105:13351-13355.
13. Namani T & Deamer D (2008) Stability of model membranes in extreme environments. *Orig. Life. Evol. Biosph.* 38:329-341.
14. Maurer SE*, et al.* (2018) Vesicle self-assembly of monoalkyl amphiphiles under the effects of high ionic strength, extreme pH, and high temperature environments. *Langmuir* 34:15560-15568.
15. Adamala K & Szostak JW (2013) Nonenzymatic template-directed RNA synthesis inside model protocells. *Science* 342:1098-1100.
16. Joyce GF & Szostak JW (2018) Protocells and RNA self-replication. *Cold Spring Harb. Perspect. Biol.* 10:a034801.
17. Longo LM & Blaber M (2012) Protein design at the interface of the pre-biotic and biotic worlds. *Arch Biochem Biophys* 526:16-21.
18. Doi N, Kakukawa K, Oishi Y, & Yanagawa H (2005) High solubility of random-sequence proteins consisting of five kinds of primitive amino acids. *Protein Eng Des Sel* 18:279-284.
19. McDonald GD & Storrie-Lombardi MC (2010) Biochemical constraints in a protobiotic earth devoid of basic amino acids: The "BAA(-) world". *Astrobiology* 10:989-1000.
20. Cleaves HJ (2010) The origin of the biologically coded amino acids. *J. Theor. Biol.* 263:490-498.
21. Black RA*, et al.* (2013) Nucleobases bind to and stabilize aggregates of a prebiotic amphiphile, providing a viable mechanism for the emergence of protocells. *Proc. Natl. Acad. Sci. U.S.A.* 110:13272-13276.
22. Black RA & Blosser MC (2016) A self-assembled aggregate composed of a fatty acid membrane and the building blocks of biological polymers provides a first step in the emergence of protocells. *Life* 6:33.
23. Adamala K & Szostak JW (2013) Competition between model protocells driven by an encapsulated catalyst. *Nature Chem.* 5:495-501.
24. Murillo-Sanchez S, Beaufils D, Gonzalez Manas JM, Pascal R, & Ruiz-Mirazo K (2016) Fatty acids' double role in the prebiotic formation of a hydrophobic dipeptide. *Chem. Sci.* 7:3406-3413.

25. Kamat NP, Tobe S, Hill IT, & Szostak JW (2015) Electrostatic localization of RNA to protocell membranes by cationic hydrophobic peptides. *Angew. Chem. Int. Ed.* 127:11901-11905.
26. Blocher M, Liu D, Walde P, & Luisi PL (1999) Liposome-assisted selective polycondensation of alpha-amino acids and peptides. *Macromolecules* 32:7332-7334.
27. Mayer C*, et al.* (2018) Molecular evolution in a peptide-vesicle system. *Life* 8:16.
28. Valeri D & Meirelles AJA (1997) Viscosities of fatty acids, triglycerides and their binary mixtures. *J. Am. Oil Chem. Soc.* 74:1221-1226.
29. Zhang W*, et al.* (2017) Quantifying binding of ethylene oxide-propylene oxide block copolymers with lipid bilayers. *Langmuir* 33:12624-12634.
30. Lindblom G, Orädd G, & Filippov A (2006) Lipid lateral diffusion in bilayers with phosphatidylcholine, sphingomyelin and cholesterol; An NMR study of dynamics and lateral phase separation. *Chem. Phys. Lipids* 141:179-184.
31. Jia L*, et al.* (2015) REDOR solid-state NMR as a probe of the membrane location of membrane-associated peptides and proteins. *J. Magn. Reson.* 253:154-165.
32. Xie L, Ghosh U, Schmick SD, & Weliky DP (2013) Residue-specific membrane location of peptides and proteins using specifically and extensively deuterated lipids and 13C-2H rotational-echo double-resonance solid-state NMR. *J. Biomol. NMR* 55:11-17.
33. Gullion T, Kishore R, & Asakura T (2003) Determining dihedral angles and local structure in silk peptide by 13C-2H REDOR. *J. Am. Chem. Soc.* 125:7510-7511.
34. Luthra SA*, et al.* (2012) Carbon-deuterium rotational-echo double-resonance NMR spectroscopy of lyophilized aspartame formulations. *J. Pharm. Sci.* 101:283-290.
35. Monnard P-A & Deamer DW (2003) Preparation of Vesicles from Nonphospholipid Amphiphiles. *Methods in Enzymology* 372:133-151.
36. Hanczyc MM, Mansy SS, & Szostak JW (2007) Mineral surface directed membrane assembly. *Orig. Life. Evol. Biosph.* 37:67-82.
37. Maurer S (2017) The impact of salts on single chain amphiphile membranes and implications for the location of the origin of life. *Life* 44:7040044-7040041 - 7040044-7040010.
38. Wang A, Miller CC, & Szostak JW (2019) Core-shell modeling of light scattering by vesicles: effect of size, contents, and lamellarity. *Biophys J.* 116:659-669.
39. Damer B & Deamer D (2015) Coupled phases and combinatorial selection in fluctuating hydrothermal pools: A scenario to guide experimental approaches to the origin of cellular life. *Life* 5:872-887.
40. Jones DD (1975) Amino acid properties and side-chain orientation in proteins: A cross correlation approach. *J. Theor. Biol.* 50:167-183.

PNAS
www.pnas.org

Supplementary Information for

Prebiotic amino acids bind to and stabilize prebiotic fatty acid membranes

Caitlin E. Cornell, Roy A. Black, Mengjun Xue, Helen E. Litz, Andrew Ramsay, Moshe Gordon, Alexander Mileant, Zachary R. Cohen, James A. Williams, Kelly K. Lee, Gary P. Drobny, and Sarah L. Keller

Corresponding authors: Roy A. Black and Sarah L. Keller
E-mail: blackr5@uw.edu and slkeller@uw.edu

This PDF file includes:

MATERIALS AND METHODS

Materials. Sodium chloride was purchased from Thermo Fisher Scientific (Waltham, MA), centrifugal filters from MilliporeSigma (Burlington, MA), and decanoic acid from Nu-Chek Prep (Elysian, MN). L-leucine ($^{13}C_6$), decanoic-10,10,10-$^{2}H_3$ acid and D_2O were from Cambridge Isotope Laboratories (Andover, MA). Decanoic-2,2-$^{2}H_2$ acid was from C/D/N Isotopes (Quebec, CA). All other chemicals were from Sigma. Except for NMR experiments, all solutions were prepared in 18 MΩ-cm water.

Decanoic acid solution. Decanoic acid was dissolved, with heating, in 190 mM NaOH to yield a 180 mM stock solution. This stock, 0.5 M monosodium phosphate, and 4 M NaCl were diluted into water to yield a solution of 50 mM decanoic acid, 30 mM sodium phosphate, and 100 mM NaCl. The pH was then adjusted to 6.83 by adding a small volume of 1 M HCl. This resulting solution is referred to as “the decanoic acid solution” and was used in all experiments except where indicated otherwise. Generally, "decanoic acid" in the text refers to mixtures of the protonated and unprotonated forms.

Diffusion NMR. Pulsed field gradient nuclear magnetic resonance (PFG-NMR) experiments were performed on a Bruker Avance III 700 MHz NMR instrument with a 5 mm Broadband Observe (BBO) probe at 25 °C. The “stebpgp1s” pulse sequence was applied to probe each amino acid's translational diffusivity (D), which was found via $\ln(I/I_0) = -\gamma^2G^2\delta^2D(\Delta-\delta/3)$. In this equation, G is the gradient strength, which varied from 10% to 95% of the maximum strength (53.5 Gauss/cm) for samples in which amino acids were in the presence of decanoic acid, and from 10% to 75% of the maximum strength for samples in the absence of decanoic acid. The variable I is the observed ^{1}H NMR peak intensity corresponding to each G, where I_0 is the intensity at the initial G value. γ is the gyromagnetic ratio of ^{1}H (4257.64 Hz/G), δ is the length of the gradient pulse (set to 0.002 s), and Δ is the diffusion time (set to 0.3 s). PFG-NMR experiments detected a series of 1D ^{1}H spectra and the diffusion coefficients were extracted by fitting the signal intensity decay at increasing gradient strengths to the equation above. Data were analyzed by extracting NMR peak intensities using the TopSpin 3.5 software package (Bruker) and exporting peak intensities to OriginPro (OriginLab, Northampton, MA), which fit the equation above and generated uncertainties of the fit. For PFG-NMR experiments, samples contained 50 mM of the amino acids leucine, glycine and serine or 10 mM lysine in the presence or absence of 50 mM deuterated decanoic acid, and were prepared in a solution of 50 mM sodium phosphate and 50 mM NaCl in D_2O at pH7 and room temperature.

REDOR. 10 mM leucine uniformly labeled with ^{13}C was mixed with 72 mM decanoic acid labeled with ^{2}H at either the 2- or 10-carbon, and ^{2}H-free water, at pH 7.6. Samples were then lyophilized and analyzed in a 11.74 T Bruker Avance III 500 MHz, narrow-bore spectrometer using a Bruker TriGamma probe tuned for ^{1}H-^{13}C-^{2}H triple resonance. The REDOR (xy-8) pulse sequence was used (1). Samples were spun at 10 kHz magic-angle spinning frequency. S0 and S1 were collected for dephasing times of 0.8, 3.2, 5.6, 8.0 and 10.4 ms and required 1024, 2048, 2048, 2048 and 4096 scans, respectively. The CP time was 1.5 ms. During this time the ^{1}H power was ramped from 70% to 100%. Field strengths were: 83 kHz ^{1}H π/2 pulse, 56 kHz ^{13}C π pulses, and 66 kHz ^{2}H π pulses. During dephasing and acquisition, 100 kHz SPINAL-64 decoupling was applied on the ^{1}H channel. Data were processed with 20 Hz Gaussian line broadening and

baseline correction. Chemical shift referencing was achieved externally using adamantane. The methylene ^{13}C shift was set to 38.5 ppm.

Filtration assay. The decanoic acid solution was added to solid base or amino acid such that the final concentration of the compound was 10 mM. The compound was ground with the end of a stirring rod to facilitate dissolution and vortexed for ~6 sec. After 30 min, 1.5 ml of solution was transferred to an Amicon Ultra-4 3K filter and centrifuged in a Beckman Allegra X-30R swinging bucket centrifuge at 3,000 *g* for 10 min at 21 °C. To assay bases (adenine and thiouracil) in the starting material and filtrate, absorbance at 260 nm was measured using an Agilent 8453 spectrophotometer, with uncertainties reported as standard error of the mean of 3 trials. To assay amino acids, (a) samples were diluted 225-fold in 0.2 M bicine at pH 9.1, (b) 750 µL of 1.5 mg/ml fluorescamine dissolved in dimethylsulfoxide was added to 315 µL of each diluted sample, and (c) after ≥ 20 min, fluorescence was measured with excitation at 400 nm and emission at 460 nm using a Perkin Elmer LS-50B fluorimeter. The assay had a standard error of ~1%.

NaCl and $MgCl_2$ effects. Methods for evaluating the flocculation of decanoic acid by NaCl are described in (2). $MgCl_2$ was added to the decanoic acid solution from a 50 mM stock solution, prior to adjusting the pH to 6.83. The resulting solution was then added to a test tube containing a solid amino acid (or to an empty test tube for the control) and vortexed briefly.

Fluorescence microscopy. This procedure was conducted as in (2); decanoic acid vesicles were labeled with the dye rhodamine 6G.

Cryo transmission electron microscopy. The decanoic acid solution was added to enough solid amino acid (or nothing for a control) to yield a 10 mM solution. After 1 min, samples were vortexed for ~6 sec. Samples were then applied to glow-discharged c-flat Holey Carbon grids (Electron Microscopy Science, Hatfield, PA) and plunge-frozen into liquid ethane using a Vitrobot Mark IV (FEI, Hillsboro, OR) at 4 °C and 100% humidity. The images were collected on a FEI T12 Spirit TEM (FEI, Hillsboro, OR) under-focused by 1.9 µm at a nominal magnification of 52,000x. Linear contrast enhancement was applied in ImageJ, a public domain program available for free download at https://imagej.nih.gov/ij/.

Turbidity. For most experiments, the decanoic acid solution was added to a test tube containing solid amino acid (or to an empty tube as control); for Fig. S7 and parts of Fig. 4B, 10 µL of a 1 M solution of amino acid in 50 mM sodium phosphate, pH 6.83 (or the buffer alone) was layered on 990 µL of the decanoic acid solution. Samples were mixed with a vortexer about one min after the addition of the solution to solid amino acid for the experiment reported in Fig. 3C. The timing of mixing in the other turbidity experiments is described in the figure legends. Turbidity values for individual samples were found as follows: each sample was plated in triplicate, and absorbance at 490 nm was measured three times with a Multiskan Spectrum microplate reader. The turbidity of that sample was taken to be the average of the nine readings, less the value of a water blank. The figures report the average of the sample values from multiple independent experiments, or, for Fig. 4B, from multiple replicate samples in one experiment. The reported standard deviations are based on these sets of values.

Critical vesicle concentration. This method is described in the legend of Fig. S10.

Critical aggregate concentration. Solutions of various decanoic acid concentrations, containing 30 mM sodium phosphate and 100 mM NaCl at pH 6.83, were added to solid amino acid such that the final amino acid concentration was 10 mM. Controls contained no amino acid. After ~30 sec, the solution was vortexed for ~6 sec. 30 min later, 8 µL of a 1 mg/mL solution of merocyanine 540 in 1:1 ethanol:water was added to 2.5 mL of the sample. Absorbance was measured with an Agilent 8453 Diode Array UV-Vis spectrophotometer from 400 nm to 700 nm, and the background at 650 nm was subtracted. The normalized intensity is reported as the intensity at 564 nm divided by the intensity at 530 nm, as detailed in (3).

Rehydration. Samples were dried in a 60 °C oven. Water was added to restore the original volume. After 30 min, samples were agitated gently by hand. After another 30 min, samples were heated for ~3 sec in an 80 °C water bath and then vortexed for ~2 sec. Absorbance at 490 nm was measured one day later with a Multiskan Spectrum microplate reader.

Size exclusion chromatography (SEC). Vesicles were prepared as described in the "Decanoic acid solutions" section above, with or without amino acids, except that 5 mM calcein was added prior to decanoic acid. Free calcein was separated from vesicles by size exclusion chromatography over a column of Sepharose 4B equilibrated with a solution of 20 mM decanoic acid, 30 mM sodium phosphate, and 100 mM NaCl, at pH 6.83. Specifically, 0.5 ml of each sample was applied to a column containing 5 ml of Sepharose 4B, and 0.5 ml fractions were collected. Vesicles elute from the columns in the first few fractions. In each experiment, one of the first four fractions was imaged by fluorescence microscopy.

Dynamic light scattering. Decanoic acid solutions were prepared with 25 mM decanoic acid (rather than 50 mM) in order to avoid multiple scattering effects. Solutions were analyzed at 25 °C on a Zetasizer Nano ZS (Malvern, Worcestershire, United Kingdom) with a 633 nm helium-neon laser using back-scattering detection (at an angle of 173° to the incident light). The average diameter and polydispersity index from the cumulant method were determined using Zetasizer software (Dispersion Technology Software version 5.00). The reported data are the averages of three runs with a single sample for each condition; variation among runs was negligible. A strong indication that the comparison is valid is that both samples had a polydispersity index of 0.3, which meets Malvern's criteria for acceptable data (4). Dynamic light scattering has been previously used as an indicator of fatty acid vesicle size (5, 6); here we used it to compare two samples rather than to determine absolute values.

Availability. All protocols are described above. All materials are commercially available, as is NMR code. Fluorescence images are original files to which only a linear contrast has been applied such that the brightest and darkest pixels span the contrast range. Other data analysis calculated only averages and associated uncertainties. Unprocessed NMR spectra and other data are available upon request to Roy Black.

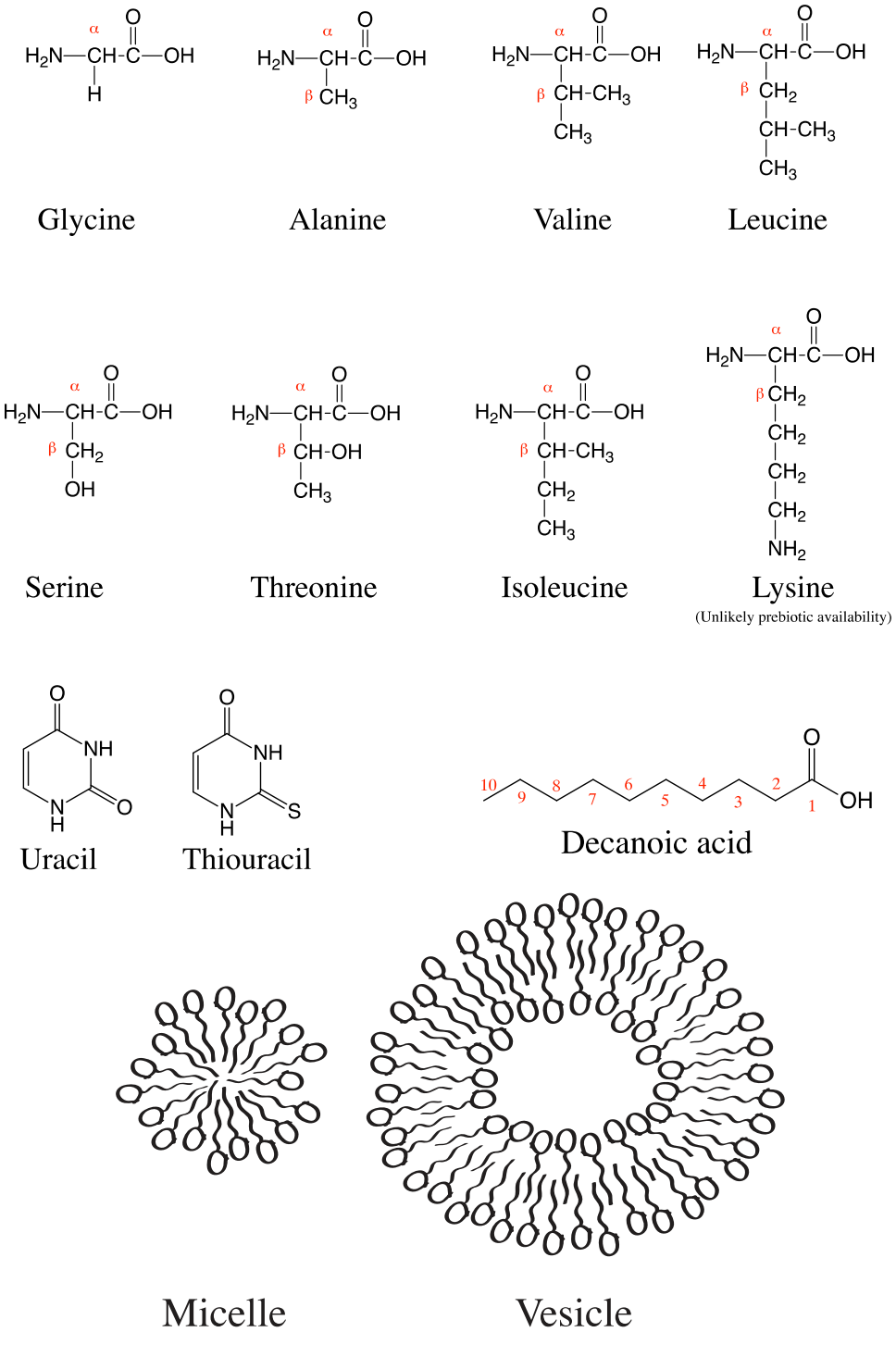

Fig. S1. Structures of amino acids, the nucleobase uracil and its related base thiouracil, decanoic acid, a micelle, and a vesicle.

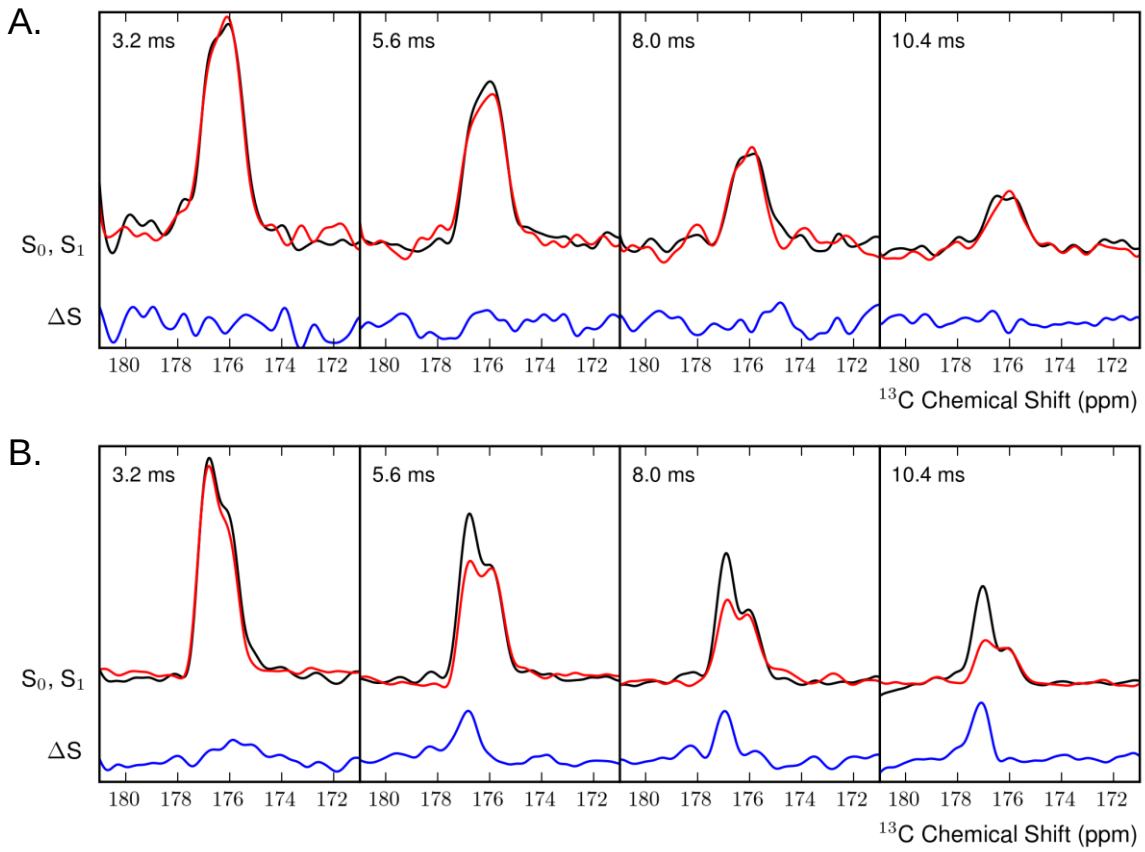

Fig. S2. Dephasing as a function of time of leucine uniformly labeled with ^{13}C. Dephasing is due to (A) decanoic acid ^{2}H-labeled at the terminal methyl group of the carbon chain (decanoic-10,10,10-$^{2}H_3$ acid) and (B) decanoic acid ^{2}H-labeled near the carbonyl group (decanoic-2,2-$^{2}H_2$ acid). The spectrum without dephasing (S0) is shown in black and the spectrum with dephasing (S1) is shown in red. ΔS is shown in blue, with a vertical offset for clarity. Note that the broad peak does not uniformly diphase. The two distinct peaks likely represent leucine molecules in two different environments: one at 177 ppm in which leucine interacts with the decanoic acid and one at 176 ppm in which it does not.

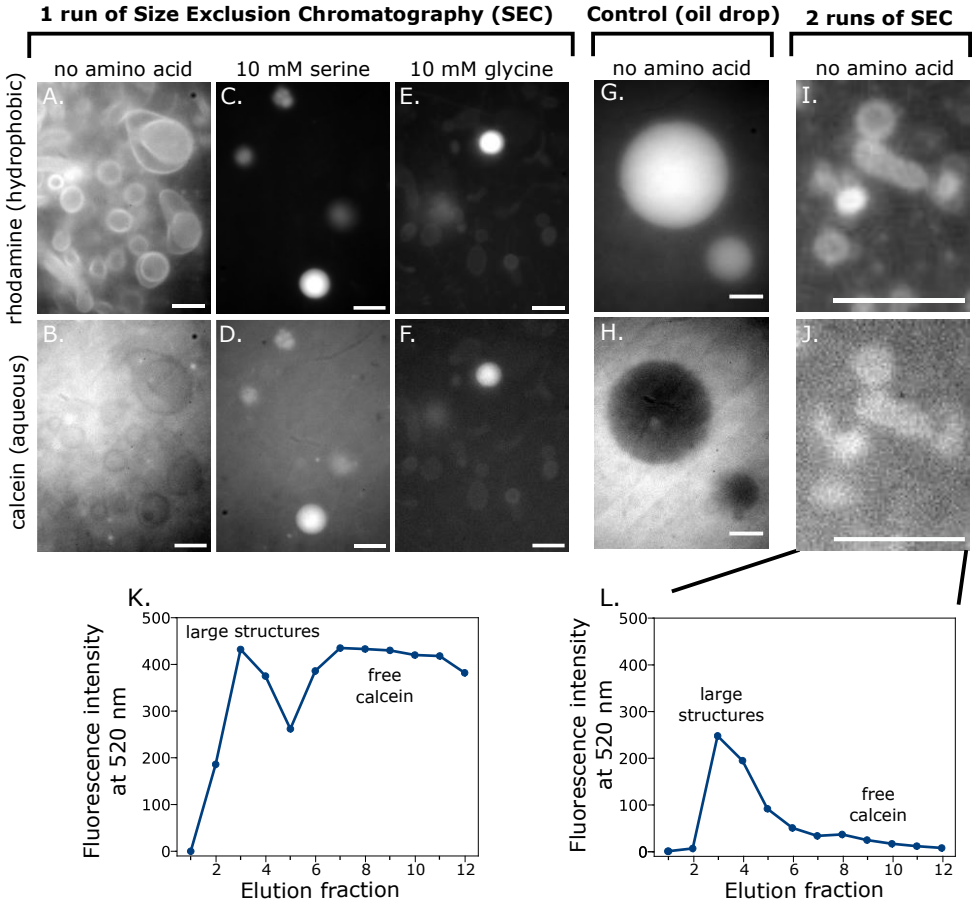

Fig. S3. Solutions of decanoic acid (with or without serine or glycine) contain individual, ~10 µm vesicles with aqueous interiors that can be labeled with calcein. Top panels show structures labeled by rhodamine 6G, a probe that labels fatty acid membranes. Bottom panels show fluorescence from calcein, a negatively-charged hydrophilic probe that does not label membranes. Calcein that was not encapsulated in vesicles was removed by running solutions through size exclusion chromatography (SEC) column(s), as described in the Methods. All scale bars are 10 µm. **A-B.** In the absence of amino acid, the decanoic acid solution contains individual, ~10 µm vesicles with membranes labeled by rhodamine 6G. After only one purification step by SEC, calcein is seen both inside and outside the vesicles. **C-F.** When 10 mM serine or glycine is included in the decanoic acid solution, bright structures are observed in both the rhodamine 6G and calcein channels, with little calcein fluorescence outside the vesicles, consistent with multilamellar vesicles that retain calcein in their interiors.

(Figure caption is continued on the next page.)

We carried out three controls to validate our SEC procedure:

1: We verified that the structures in Panels A-F are inconsistent with oil droplets.
2: We confirmed that the interiors of the vesicles in Panels A-B are aqueous.
3: We verified that our size-exclusion chromatography separates vesicles from calcein.

G-H. Control 1: We lowered the pH of the calcein-containing decanoic acid solution to 6.3 to induce the formation of oil droplets. Panel G shows that oil droplets are labeled by rhodamine 6G, and Panel H shows that calcein is excluded from oil droplets.
I-J. Control 2: We ran a calcein-containing decanoic acid solution over a SEC column, merged fractions 3 and 4, ran 0.5 mL of this pool over a second SEC column to further remove excess free calcein, and then analyzed early-eluting fractions from the second run by fluorescence microscopy. As observed after only one run (Panels A-B), vesicle membranes were labeled by rhodamine 6G and the lumen was labeled by calcein. As expected, the second SEC run removed more unencapsulated calcein such that the calcein fluorescence inside the vesicles became clearly greater than outside the vesicles (unlike in panel B). The vesicles that emerged from the second SEC run were consistently smaller than after the first run.
K-L. Control 3: We measured the fluorescence intensity due to calcein (at 520 nm) for each fraction eluted from the first (Panel K) and second (Panel L) SEC runs described within Control 2. To eliminate any vesicles that might affect calcein fluorescence, the data in Panels K-L were collected after adding NaOH to each sample (to a final concentration of 1 M), which converts decanoic acid vesicles to decanoate micelles. After the first SEC run, total fluorescence from free calcein in solution appeared higher than the fluorescence associated with vesicles. After the second SEC run, the level of free calcein in solution was much lower than the level in vesicles.

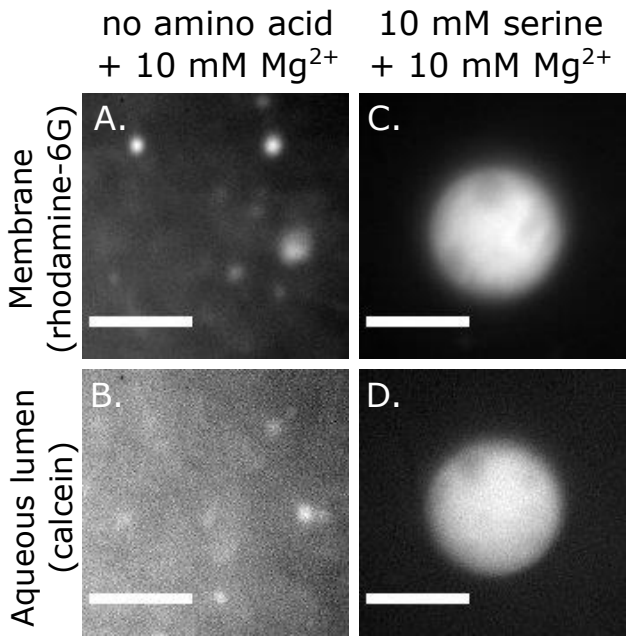

Fig. S4. Individual, ~10 μm decanoic acid vesicles with serine are not disrupted by 10 mM Mg^{2+}; they retain calcein in their lumens. Vesicle solutions were prepared as described in the Methods, except that 5 mM calcein was added before the decanoic acid. The pH of the solutions was then adjusted to 6.83 and serine was either added (to a final concentration of 10 mM) or not. Next, $MgCl_2$ was added to a concentration of 10 mM, the solutions were briefly vortexed, and the pH was re-adjusted to 6.83.

Free calcein was separated from vesicles by size exclusion chromatography as described in the Methods, and early-eluting fractions were used for fluorescence microscopy. Top panels show structures labeled by rhodamine 6G, a probe that labels decanoic acid membranes, and bottom panels show fluorescence due to calcein, a negatively-charged, hydrophilic probe. **A-B.** In the absence of serine, only small structures are observed. In some cases, these structures are labeled by both rhodamine 6G and calcein, which suggests that at least some of the structures are vesicles. However, few of the vesicles approach 1 μm in size, and the poor correspondence between structures labeled with rhodamine 6G and calcein implies that the membranes allow significant leakage of vesicle contents. **C-D.** In the presence of both serine and Mg^{2+}, ~10 μm structures are observed that are labeled by both rhodamine 6G and calcein. These structures are indistinguishable from those prepared in the absence of Mg^{2+} (compare to SI Appendix, Fig. S3 C-D). Scale bars are 10 μm.

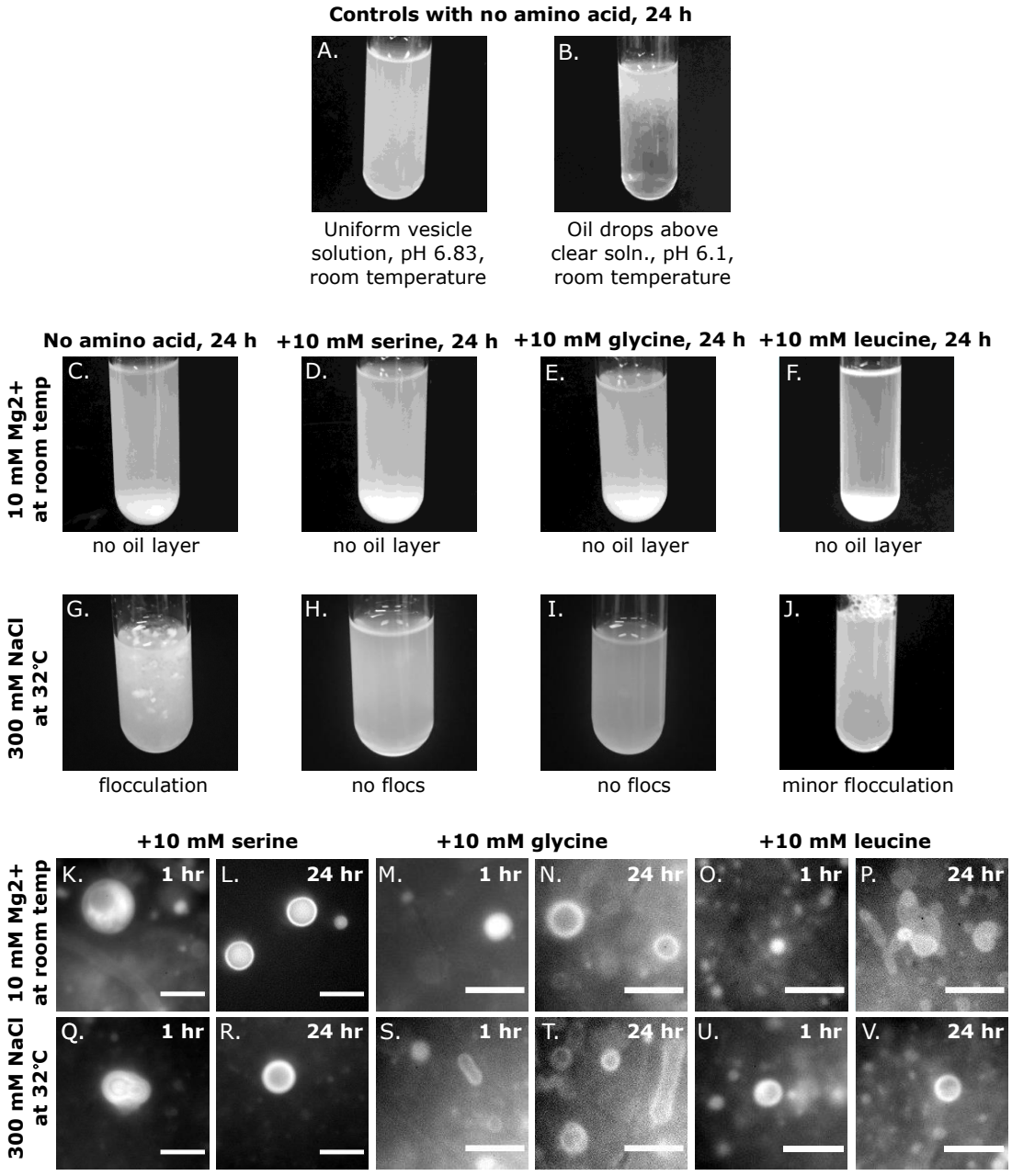

Fig. S5. No millimeter-scale or micron-scale evidence of oil droplets appears in solutions of decanoic acid at pH 6.83, whether or not the solutions contain amino acids (serine, glycine, or leucine). All samples containing NaCl were prepared with 80 mM decanoic acid at pH 7.65, as in reference 2. NaCl was added at room temperature, and then the samples were brought to 32 ˚C, where they remained for the duration of the experiment. In the images, all test tubes are 13 mm wide and were photographed with an iPhone camera under ambient light.

(Figure caption is continued on the next page.)

Millimeter-scale Behavior: A. Decanoic acid solutions at pH 6.83 appear uniformly cloudy because they contain paucilamellar micron-scale vesicles. **B.** Shifting the pH to 6.1 causes oil droplets of decanoic acid to form. When solutions with oil droplets are allowed to sit for 24 h, the bottom half of the solutions becomes relatively clear because oil droplets have floated to the top of the test tube. **C-F.** The appearance of solutions containing 10 mM Mg^{2+} is inconsistent with the formation of oil droplets: the solution at the bottom of the test tubes is not more clear than at the top. Mg^{2+} destabilizes individual, ~10 μm vesicles (Fig. 2). Mg^{2+} also appears to cause some precipitate to form at the bottom of the test tubes. **G-J.** The appearance of solutions containing 300 mM NaCl is also inconsistent with the formation of oil droplets: the solution at the bottom of the test tubes is not more clear than at the top. In Panel G, millimeter-scale flocs are observed, and reduced flocculation is seen in Panel J.

Micrometer-scale Behavior: All samples contain rhodamine 6G, a fluorophore that labels decanoic acid membranes and oil droplets. All scale bars on fluorescence micrographs are 10 μm. **K-N, Q-V.** In solutions containing serine, glycine, or leucine, with Mg^{2+} or NaCl as indicated, micron-scale structures persist after 24 h without significantly increasing in size. The lumens of at least some of the structures are not labeled by rhodamine 6G, in contrast to oil droplets, which have interiors labeled by this dye (SI Appendix, Fig. S3, Panel G) and should coalesce over time. **O-P.** In solutions containing Mg^{2+} and leucine, vesicles with distinct lumens appear after 24 h.

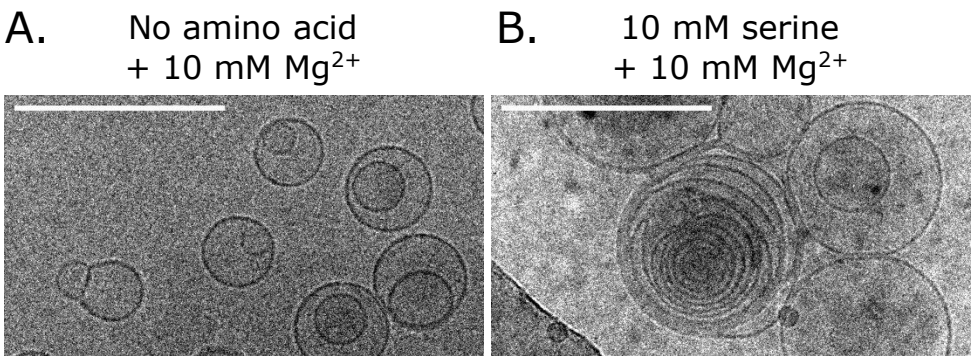

Fig. S6. Cryo TEM shows that with serine present, multilamellar vesicles persist in the presence of 10 mM Mg^{2+}. A. No amino acid added. B. 10 mM serine added. Cryo TEM records images of vesicles that are smaller than vesicles seen in fluorescence micrographs because vesicles larger than 300 nm are not retained on TEM grids. Vesicles less than 50 nm in diameter persist in the presence of 10 mM Mg^{2+} even without addition of any amino acid; these vesicles would be unresolvable by fluorescence microscopy. Scale bars are 100 nm.

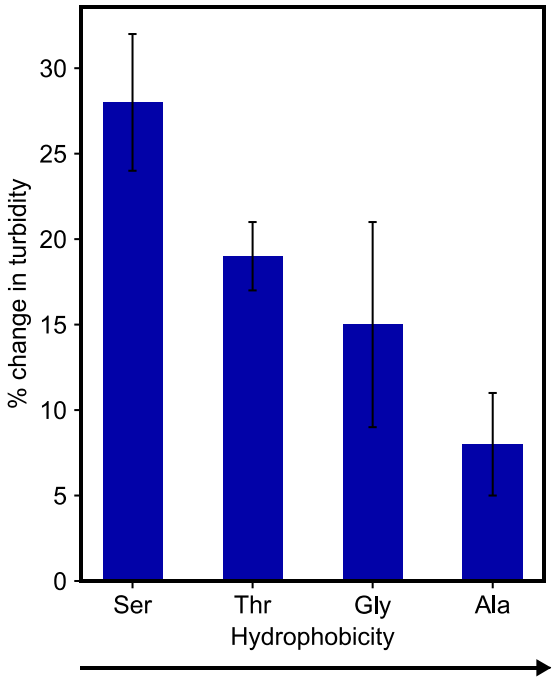

Fig. S7. Amino acids increase the turbidity (the absorbance at 490 nm) of the decanoic acid solution when added as concentrated solutions. 10 µL of a 1 M solution of each amino acid in 50 mM sodium phosphate at pH 6.83 ± 0.03 was overlaid on 990 µL of a solution that contained 50 mM decanoic acid, 30 mM sodium phosphate, and 100 mM NaCl at pH 6.83. Twenty seconds later, the sample was vortexed for ~6 seconds. For a control, 10 µl of the same phosphate buffer (with no amino acid) was added. The relative effectiveness of the amino acids, with diminished turbidity for more hydrophobic amino acids, is similar to that seen when the amino acids are added as solids (c.f. Fig 3C in the main text).

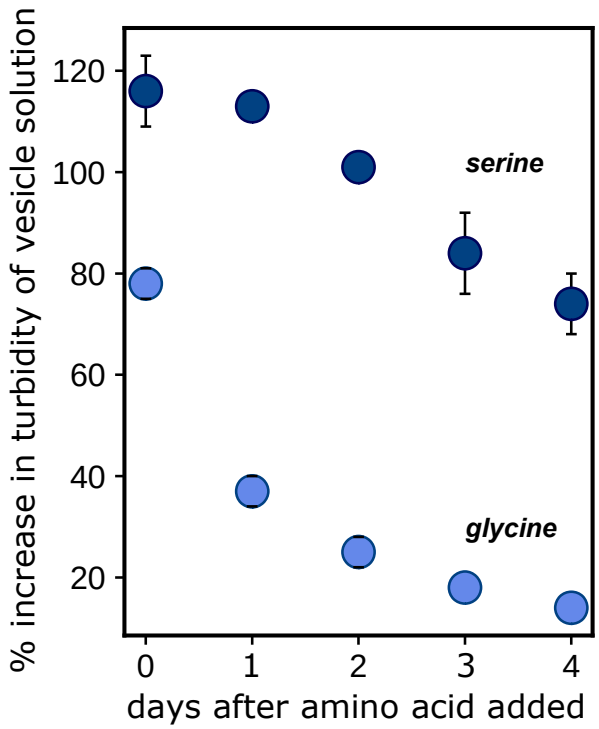

Fig. S8. The increase in turbidity in decanoic acid solutions caused by the addition of serine and glycine decays over a period of days. The decanoic acid solution was added to solid amino acid such that the resulting solution contained 10 mM amino acid, or to an empty tube as a control. One minute later, samples were vortexed for ~6 seconds. Turbidity (absorbance at 490 nm) of the samples was determined 30 minutes later and then daily. The figure records the percentage change of the test with respect to the control. Three experiments were conducted: one extended through Day 2 and two extended through Day 4. Standard errors of the mean are shown for Days 0, 1, and 2, and average errors are shown for Days 3 and 4, unless the errors are smaller than the symbols.

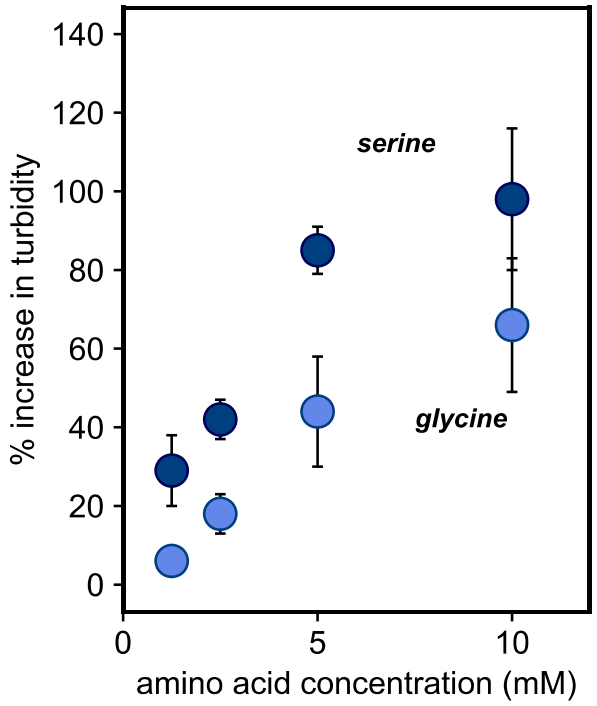

Fig. S9. At concentrations of 1.25 mM and higher, amino acids serine and glycine significantly increase turbidity of solutions containing decanoic acid vesicles, and the effect increases with concentration of the amino acid. The decanoic acid solution was added to a test tube containing solid amino acid such that the final amino acid concentration was 0, 1.25, 2.5, 5 or 10 mM. One minute after each addition, samples were vortexed for ~6 seconds. Turbidity, measured by absorbance at 490 nm, was determined 30 minutes later. The graph shows the percent increase in turbidity relative to the control with no amino acid. Each point is the average of at least three experiments. Error bars denote standard deviations, including when the error is smaller than the symbol size.

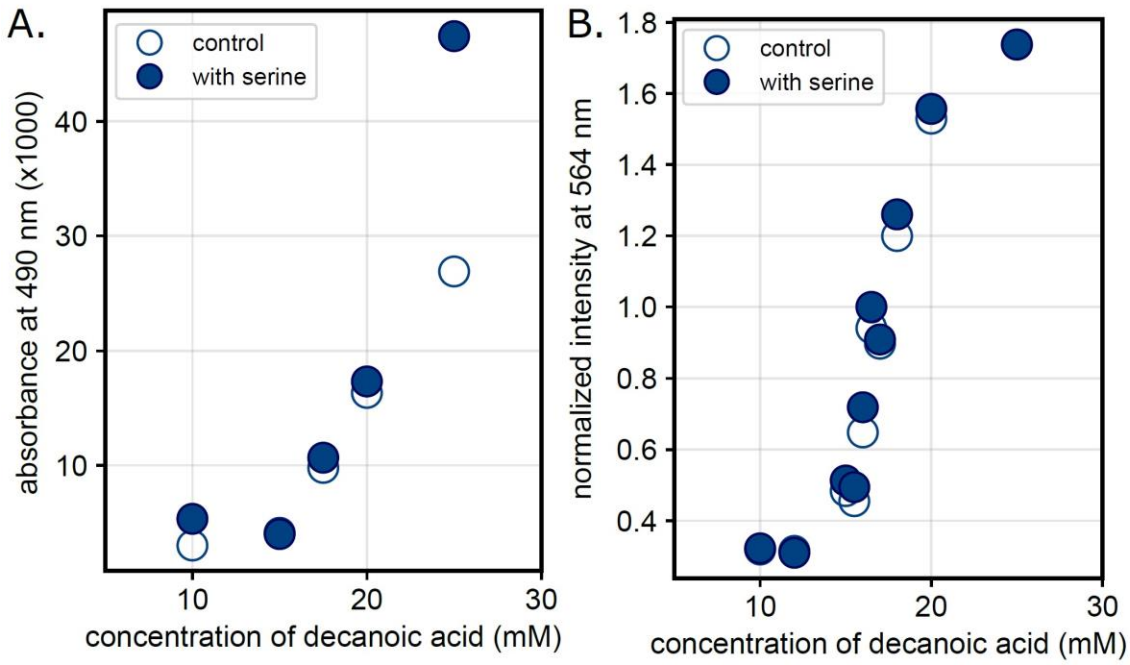

Fig. S10. Serine does not affect the critical vesicle concentration of decanoic acid solutions, as determined by two methods. **A.** Solutions containing 25 mM decanoic acid, 30 mM sodium phosphate, and 100 mM NaCl at pH 6.83, with and without 10 mM serine, were diluted until the concentration of decanoic acid was as low as 10 mM. The diluting solution contained all of the same compounds except decanoic acid. The critical vesicle concentration was identified as a sharp change in the absorbance of the sample at 490 nm. **B.** The critical vesicle concentration was measured via an assay that employs merocyanine 540, a dye. The absorption spectrum of this dye shifts in hydrophobic environments, including surfactant aggregates (7). Solutions containing 10-25 mM decanoic acid with or without 10 mM serine were prepared as in the Methods. At least 30 min later, 8 µL of 1 mg/mL merocyanine 540 that had been dissolved in 1:1 water:ethanol was added to 2.5 mL of each decanoic acid solution. The critical aggregate concentration was measured as in (3). Briefly, each sample's absorbance was measured at 530, 564, and 630 nm (denoted A_{530}, A_{564}, and A_{630}). The critical aggregate concentration was identified by a sharp change in the quantity: $(A_{564} - A_{630})/(A_{530} - A_{630})$.

Table. S1. Summary of Results.

	Lys	Ser	Thr	Gly	Ala	Val	Leu	Ile		Fig
		(These seven amino acids are considered prebiotic.)								
BIND MEMBRANE	**Diffusion NMR**	**Yes**	**Yes**	**–**	**Yes**	**–**	**–**	**Yes**	**–**		**1B**
	Strength of evidence	Strong	Strong	–	Strong	–	–	Strong	–		
	Retention w/ vesicles	**–**	**Maybe**	**Maybe**	**Maybe**	**Yes**	**Yes**	**Yes**	**Yes**		**1C**
	Strength of evidence	–	Error bars overlap control	Error bars overlap control	Error bars overlap control	Clearly exceeds control	Clearly exceeds control	Clearly exceeds control	Clearly exceeds control		
PROTECT ~10 µm VESICLE OR INCREASE # LAMELLAE	**Cryo TEM w/ more layers**	**–**	**Yes**	**–**	**–**	**–**	**–**	**–**	**–**		**3**
	Strength of evidence	–	Strong	–	–	–	–	–	–		
	Increase in brightness	**–**	**Yes**	**–**	**Yes**	**–**	**–**	**No**	**–**		**2 & 3**
	Strength of evidence	–	Strong	–	Strong	–	–	Strong	–		
	Protects vs. 10mM Mg2+	**–**	**Yes**	**–**	**Yes**	**–**	**–**	**No**	**–**		**2, S4 & S5**
	Strength of evidence	–	Strong	–	Strong	–	–	Strong	–		
	Protects vs. 300 mM NaCl	**–**	**Yes**	**–**	**Yes**	**–**	**–**	**Some**	**–**		**2 & S5**
	Strength of evidence	–	Strong	–	Strong	–	–	Strong	–		
	Increase in turbidity	**–**	**Yes**	**Yes**	**Yes**	**Yes**	**No**	**No**	**No**		**3**
	Strength of evidence	–	Strong data. Indirect result likely due to more lamellae	Strong data. Indirect result likely due to more lamellae	Strong data. Indirect result likely due to more lamellae	Strong data. Indirect result likely due to more lamellae	Strong data. Indirect result likely due to more lamellae	Strong data. Indirect result likely due to more lamellae	Strong data. Indirect result likely due to more lamellae		

Table. S2. Diffusion coefficients of amino acids and water in solutions without and with decanoic acid.

		Diffusion Coefficient (m^2/s)		
		fast	**slow**	**water**
Samples *without* decanoic acid vesicles	Glycine	$7.6445\times10^{-10} \pm 1.6\times10^{-13}$	none	$1.69715\times10^{-9} \pm 3.7\times10^{-13}$
	Leucine Trial 1	$5.20932\times10^{-10} \pm 8.4\times10^{-14}$	none	$1.67917\times10^{-9} \pm 2.8\times10^{-13}$
	Leucine Trial 2	$5.21152\times10^{-10} \pm 7.4\times10^{-14}$	none	$1.68409\times10^{-9} \pm 3.1\times10^{-13}$
	Serine	$6.3733\times10^{-10} \pm 3.86\times10^{-13}$	none	$1.69553\times10^{-9} \pm 5.7\times10^{-13}$
	Lysine	$4.8876\times10^{-10} \pm 5.8\times10^{-13}$	none	$1.70501\times10^{-9} \pm 2.0\times10^{-13}$
Samples *with* decanoic acid vesicles	Glycine	$7.3974\times10^{-10} \pm 2.4\times10^{-13}$	$1.04\times10^{-12} \pm 3.1\times10^{-13}$	$1.59499\times10^{-9} \pm 3.3\times10^{-13}$
	Leucine Trial 1	$4.9420\times10^{-10} \pm 1.5\times10^{-13}$	$2.98\times10^{-12} \pm 1.9\times10^{-13}$	$1.52258\times10^{-9} \pm 2.8\times10^{-13}$
	Leucine Trial 2	$4.9601\times10^{-10} \pm 1.33\times10^{-13}$	$2.98\times10^{-12} \pm 1.8\times10^{-13}$	$1.53912\times10^{-9} \pm 1.9\times10^{-13}$
	Serine	$6.1322\times10^{-10} \pm 6.3\times10^{-13}$	$1.76\times10^{-12} \pm 1.07\times10^{-12}$	$1.5932\times10^{-9} \pm 5\times10^{-13}$
	Lysine	$4.580\times10^{-10} \pm 1.7\times10^{-12}$	$1.03\times10^{-11} \pm 2.1\times10^{-12}$	$1.56629\times10^{-9} \pm 2.0\times10^{-13}$

SI REFERENCES

1. McDowell LM, Holl SM, Qian S, Li E, & Schaefer J (1993) Inter-tryptophan distances in rat cellular retinol binding protein II by solid-state NMR. *Biochemistry* 32:4560-4563.
2. Black RA, *et al.* (2013) Nucleobases bind to and stabilize aggregates of a prebiotic amphiphile, providing a viable mechanism for the emergence of protocells. *Proc. Natl. Acad. Sci. U.S.A.* 110:13272-13276
3. Maurer S & Nguyen G (2016) Prebiotic vesicle formation and the necessity of salts. *Orig. Life. Evol. Biosph.* 46:215-222.
4. http://149.171.168.221/partcat/wp-content/uploads/Malvern-Zetasizer-LS.pdf, accessed 20 June 2019.
5. Blöchliger E, Blocher M, Walde P & Luisi PL (1998) Matrix effect in the size distribution of fatty acid vesicles. *J. Phys. Chem. B.* 102: 10383-10390.
6. Markvoort AJ, Pfeger N, Staffhorst R, Hilbers PAJ, van Santen RA, Killian JA, & de Kruijff B (2010) Self-reproduction of fatty acid vesicles: A combined experimental and simulation study. *Biophys. J.* 99: 1520-1528.
7. Dixit NS & Mackay RA (1983) Absorption and emission characteristics of merocyanine-540 in microemulsions. *J. Am. Chem. Soc.* 105:2928-2929.